INSTITUTE OF PHYSICS PUBLISHING JOURNAL OF PHYSICS: CONDENSED MATTER

J. Phys.: Condens. Matter **15** (2003) L139–L145 PII: S0953-8984(03)57558-0

LETTER TO THE EDITOR

Raman scattering study of charge ordering in β-$Ca_{0.33}V_2O_5$

Z V Popović[1,3], M J Konstantinović[1], V V Moshchalkov[1], M Isobe[2] and Y Ueda[2]

[1] Laboratorium voor Vaste-Stoffysica en Magnetisme, Katholieke Universiteit Leuven, Celestijnenlaan 200D, B-3001 Leuven, Belgium
[2] Materials Design and Characterization Laboratory, Institute for Solid State Physics, The University of Tokyo, 5-1-5 Kashiwanoha, Kashiwa, Chiba 277-8581, Japan

E-mail: Zoran.Popovic@uv.es

Received 17 December 2002
Published 3 February 2003
Online at stacks.iop.org/JPhysCM/15/L139

Abstract
Polarized Raman spectra of the calcium vanadium oxide bronze β-$Ca_{0.33}V_2O_5$ are measured in the temperature range between 300 and 20 K. The charge ordering phase transition at about 150 K is characterized by the appearance of new Raman-active modes in the spectra, and by anomalies in the electronic background scattering. The high-temperature Raman scattering spectra of β-$Ca_{0.33}V_2O_5$ show an apparent resemblance to those of α'-NaV_2O_5, which suggests that the charge–phonon dynamics of the two compounds are similar. A study of the dynamical properties and a symmetry analysis of the Raman modes show that in the mixed-valence state of β-$Ca_{0.33}V_2O_5$ the electrons are delocalized into V_1–O_5–V_3 orbitals. We propose that in the charge ordered state below 150 K the d electrons localize within V_1–V_3 ladders, either in a 'zigzag' fashion as in α'-NaV_2O_5 or in the form of double chains as in γ-LiV_2O_5.

(Some figures in this article are in colour only in the electronic version)

The vanadium bronzes, β (β')-$A_x^{1+\,(2+)}V_2O_5$ ($x = \frac{1}{3}, \frac{2}{3}$; A = Li, Na, Ag, Ca, Sr, Pb, Cu etc), exhibit a variety of phenomena that originate from strong electron correlations. For example, various charge and spin orderings [1–4], and even superconductivity (β-$Na_{0.33}V_2O_5$ [5] and β'-$Cu_{0.65}V_2O_5$ [6]), are found in this class of materials. The electronic properties are not yet fully understood due to the complex crystal structure of these bronzes. The β-compounds with divalent A cations such as Ca^{2+} and Sr^{2+} were first prepared by Bouloux *et al* [7]. X-ray measurements [8] revealed the presence of a superstructure with a lattice modulation vector $\vec{q} = (0, 1/2, 0)$ at room temperature in β-$A_{0.33}^{2+}V_2O_5$ (A = Ca and Sr). This indicates doubling

[3] Present address: Materials Science Institute, University of Valencia, Poligono La Coma s/n, 46980 Paterna (Valencia), Spain.

of the unit cell along the b-axis. Such a superstructure was also observed in β-$A^{1+}_{0.33}V_2O_5$ (A = Na and Ag) [8] below room temperature, originating from the ordering of the A cations along the b-axis—that is, formation of A chains where the A cations and vacancies alternate with each other.

The magnetic susceptibility of β-$Ca_{0.33}V_2O_5$ versus temperature, $\chi(T)$, shows a slight jump at around 150 K [8], indicating the existence of a phase transition. Above the transition temperature the magnetic susceptibility is almost temperature independent, whereas below the transition temperature it shows a low-dimensional behaviour. The magnetic susceptibility has a maximum around 50 K, then decreases further on reducing the temperature, but shows an upturn at lower temperatures which is caused by impurities or defects [8]. At the transition, the lattice parameters show a discontinuous change, typical for a first-order transition. The NMR study [9] has revealed that above the transition temperature there is only one kind of electronic state of the V site, whereas below the transition temperature $T = T_{CO} = 149$ K one finds two kinds of V site which can be identified as magnetic V^{4+} and nonmagnetic V^{5+}. This finding strongly suggests the existence of a CO transition or the appearance of a charge disproportionation at T_{CO}.

Here we analyse the CO phase transition in β-$Ca_{0.33}V_2O_5$ using the Raman scattering technique. First, we show that CO in β-$Ca_{0.33}V_2O_5$ causes changes in the phonon spectra similar to those found in α'-NaV_2O_5. Second, we discuss the electron localization effects and possible CO patterns in this bronze.

Powder samples of β-$Ca_{0.33}V_2O_5$ were prepared by solid-state reaction of mixtures with an appropriate molar ratio of $Ca_2V_2O_7$, V_2O_3, and V_2O_5. The mixtures were pressed into pellets and heated at 650 °C in an evacuated silica tube for several days with some intermediate grindings. Details of the sample preparation were published in [8].

The crystal structure of the β-phase is monoclinic, space group $C2/m$ (C^3_{2h}), with $Z = 6$ formula units per unit cell. It has a characteristic V_2O_5 framework formed by the edge/corner-sharing VO_5 and VO_6, as shown in figure 1(a). There are three different sites for vanadium atoms: V_1, V_2, and V_3. The V_2O_5 framework consists of three kinds of infinite double chain along the b-axis, as shown in figure 1(b). The V_1 sites have sixfold, octahedral coordination and form a zigzag chain by sharing the edges of the VO_6 octahedra. The V_2 sites with similar octahedral coordination form a ladder chain by sharing corners, and the V_3 sites, which have fivefold, square pyramidal coordination, form a zigzag chain by sharing the edges. The Ca cations are located at the sites in the tunnel formed by the V_2O_5 framework. There are two equivalent sites for Ca, but two Ca sites at the same height along the b-axis cannot be occupied simultaneously. Therefore, the stoichiometric composition can be expressed as $Ca_{1/3}V_2O_5$, that is, CaV_6O_{15}.

The Raman spectra were measured for very small crystals of typical size 5×15 μm embedded in the powder pellets. We used a micro-Raman system with a DILOR triple monochromator including a liquid-nitrogen-cooled charge-coupled-device detector. The 514.5 nm line of an Ar-ion laser was used as the excitation source. Low-temperature measurements we carried out in an Oxford continuous flow cryostat with a 0.5 mm thick window. The laser beam was focused by a long-distance (10 mm focal length) microscope objective (magnification 50×).

The β-$Ca_{0.33}V_2O_5$ unit cell consists of six formula units ($Z = 6$) with 44 atoms in all. Because of that we can expect a large number of optically active modes. All atoms (except O_1, which has the C_{2h} site symmetry) have the 4(i) position symmetry of the $C2/m$ (C^3_{2h}) space group [10]. Factor-group analysis (FGA) yields the following distribution of vibrational modes:

$$\Gamma = 20A_g(xx, yy, zz, xz) + 10B_g(xy, yz) + 12A_u(\boldsymbol{E} \parallel \boldsymbol{y}) + 24B_u(\boldsymbol{E} \parallel \boldsymbol{x}, \boldsymbol{E} \parallel \boldsymbol{z}).$$

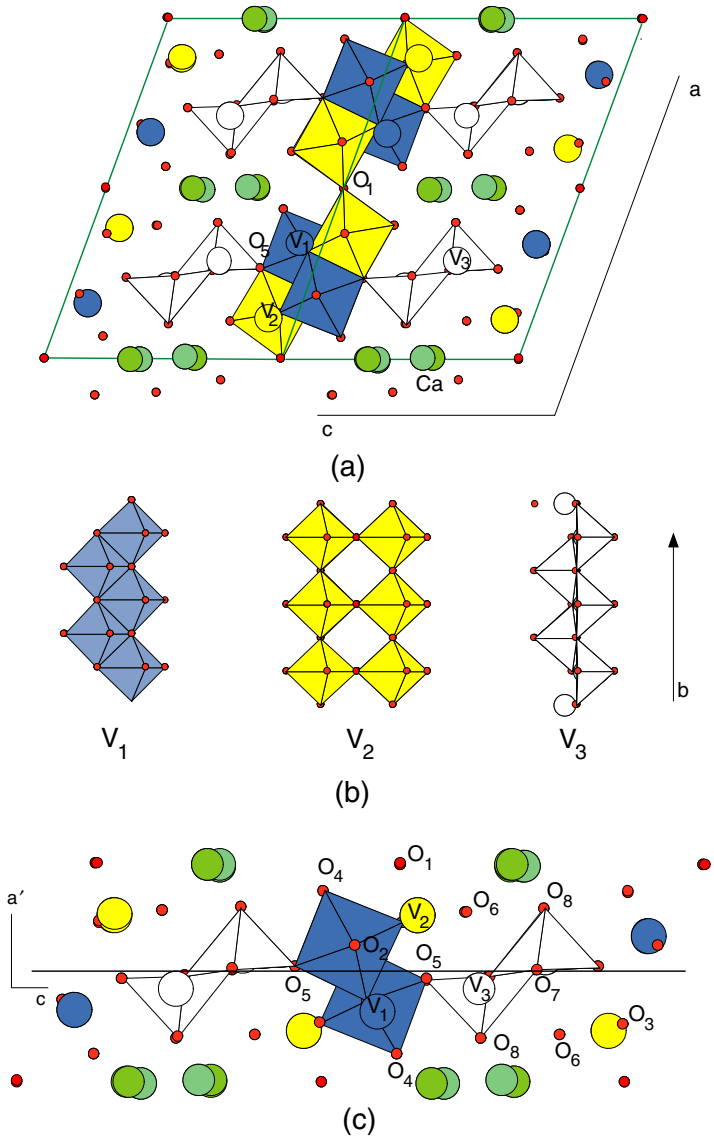

Figure 1. (a) The crystal structure of β-$Ca_{0.33}V_2O_5$ projected on the (ac) plane. (b) Three types of V chain running parallel to the b-axis. (c) A schematic representation of the up–up–down–down orientation of the VO_5 and VO_6 polyhedra along the c-axis.

According to this representation, one can expect 30 Raman-and 33 infrared-active modes ($1A_u$ and $2B_u$ are acoustic modes).

The polarized Raman spectra of β-$Ca_{0.33}V_2O_5$, measured from the (bc) plane at room temperature, for the parallel and crossed polarizations, are given in figure 2 together with the polarized Raman spectra of α'-NaV_2O_5. We find that these spectra coincide with each other in many details, which suggests structural similarities and similarities in the normal coordinates of the vibrational modes, as we will discuss later. The spectra for parallel polarizations consist of the A_g symmetry modes. Nine modes, at 114, 129, 228, 307, 335, 441, 508, 556, and 978 cm^{-1}, are clearly seen for the (cc) polarization and five additional modes, at 156, 247,

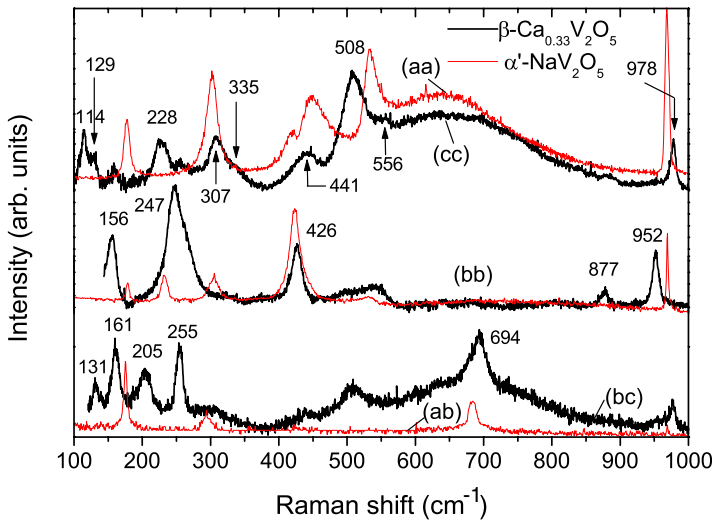

Figure 2. Room temperature polarized Raman spectra of β-$Ca_{0.33}V_2O_5$, together with the corresponding Raman spectra of α'-NaV_2O_5. $\lambda_L = 514.5$ nm.

426, 877, and 952 cm^{-1}, are seen for the (*bb*) polarization. For the crossed (*bc*) polarization, five Raman-active B_g symmetry modes, at 131, 161, 205, 255, and 694 cm^{-1}, are observed. As was already discussed for the case of AV_2O_5 [11, 12], the phonon modes in the spectral range below 500 cm^{-1} originate from the bond bending vibrations, whereas the higher-frequency modes originate from the stretching vibrations of the V–O ions. The highest-frequency mode at 978 cm^{-1} represents V_3–O_8 (see figure 1) stretching vibrations (V–O_1 bond stretching vibration in sodium vanadate [11]), whereas the modes at about 877 and 952 cm^{-1} originate from V_2–O_6 and V_1–O_4 bond stretching vibrations, respectively. These modes appear at the highest frequencies, because they arise from the shortest V–O bonds (V_3–O_8 in the VO_5 pyramid, V_2–O_6 and V_1–O_4 bonds in the VO_6 octahedra; see figure 1). Note that the V–O bond stretching vibrational modes in the octahedral surroundings have lower frequencies than in the pyramidal surroundings, as already found in [13].

The B_{1g} symmetry mode at 694 cm^{-1} corresponds to the bond stretching vibrations of V_3 and O_7 ions along the *b*-axis. Since the V–O_2 distance in β-$Ca_{0.33}V_2O_5$ is close to the same distance (V–O_{2b}) in α'-NaV_2O_5, there is no significant mode frequency difference between these two oxides. The next A_{1g} mode of β-$Ca_{0.33}V_2O_5$ appears at a frequency of 508 cm^{-1}. The frequency of the analogous mode in α'-NaV_2O_5 is 534 cm^{-1}. This mode represents the bond stretching vibration of V_3 and O_7 ions, along the *c*-axis. The frequency difference between these modes is in accordance with the difference between values of the V_3–O_{7c} bond lengths in β-$Ca_{0.33}V_2O_5$ (2.0 Å) and V–O_{2a} in α'-NaV_2O_5 (1.985 Å).

The Raman mode at 448 cm^{-1} in α'-NaV_2O_5 is related to the V–O_3–V bending vibrations [11] (mostly vibrations of oxygen ions in the rungs of the ladder structure of sodium vanadate along the *c*-axis direction). As we discussed in [11, 12], the force constant of this mode is strongly affected by the charge of the electrons in the rung. Because of that, this mode appears at a frequency below its intrinsic value of 485 cm^{-1} in pure V_2O_5 or 470 cm^{-1} in CaV_2O_5 (where spin electrons are attached to the V^{4+} ions) [11]. In addition, this mode in α'-NaV_2O_5 shows strong asymmetry and broadening. Since this mode has the same shape and position in α'-NaV_2O_5 and β-$Ca_{0.33}V_2O_5$, we conclude that the electrons in β-Ca vanadate bronze are also delocalized in the V–O–V orbitals, where the O denotes corner oxygen ions

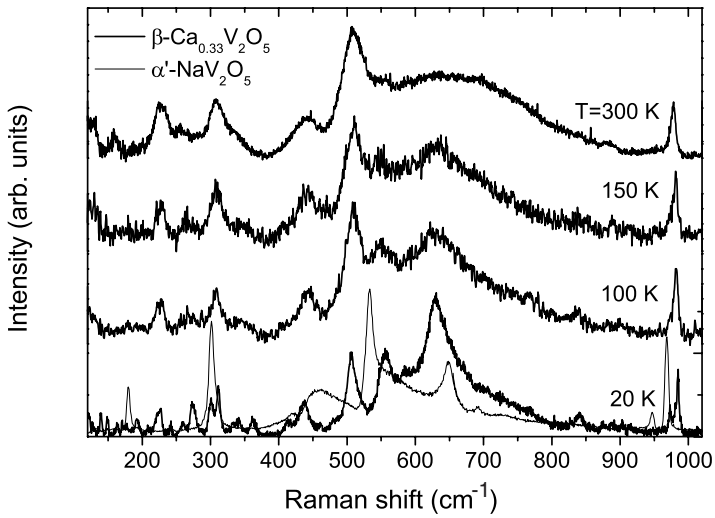

Figure 3. The (cc)-polarized Raman spectra of β-$Ca_{0.33}V_2O_5$ at different temperatures. The thin curve shows the (aa)-polarized spectrum of α'-NaV_2O_5 at $T = 20$ K.

common to the $VO_{5(6)}$ polyhedra. There are two bridge oxygens in different $VO_{5(6)}$ polyhedra: O_1 and O_5 (figure 1). Since O_1 is at a centre of inversion, its vibration does not contribute to the Raman scattering process. Thus, only the O_5-ion vibration can be included in the normal coordinate of the 441 cm^{-1} V–O–V mode. Furthermore, there are three possible V–O_5–V bonds for the normal coordinate of the 441 cm^{-1} mode: V_2–O_5–V_1, V_2–O_5–V_3, and V_1–O_5–V_3. Since only the V_1–O_5–V_3 bond has nearly the same bond length (3.74 Å) and bond angle (136°) as in α'-NaV_2O_5 [11], we conclude that the 441 cm^{-1} mode corresponds to the V_1–O_5–V_3 bond bending vibration. This means that although V_1 and V_3 are V ions at different sites, they are in the mixed-valence state ($V^{4.5+}$), whereas the V_2 are all in 5+ states at room temperature. The crystallographic similarity between α'-NaV_2O_5 and β-$Ca_{0.33}V_2O_5$ is illustrated in figure 1(c). Note that the VO_5 pyramids and VO_6 octahedra are oriented along the c-axis in an 'up–up–down–down' pattern in β-$Ca_{0.33}V_2O_5$ similar to the VO_5 pyramidal structure along the a-axis in α'-NaV_2O_5.

Figure 3 shows the Raman spectra of β-$Ca_{0.33}V_2O_5$ for the (cc) polarization at different temperatures. On lowering the temperature all observed modes harden and two new modes at 555 and 630 cm^{-1} appear from the broad structure peaked at about 650 cm^{-1}. These two modes become more pronounced below the transition temperature (150 K), and they are the most intense ones at the lowest temperature, of about 20 K, that we used in our experiments. At temperatures less than 100 K almost all modes split as a consequence of charge ordering followed by the doubling of the unit cell. This causes the appearance of zone boundary modes in the Raman spectra.

In the charge ordered phase there are two possible ways to redistribute the d electrons from the V_1–O_5–V_3 orbitals:

(i) Below T_{CO}, the spin electrons from the V_1–O_5–V_3 orbitals localize at the V_1 and V_3 sites, forming a zigzag ordering pattern similar to that of the low-temperature phase of α'-NaV_2O_5; figure 4(a).

(ii) The spin electrons from the V_1–O_5–V_3 orbitals localize at the V_1 ions forming a 1D magnetic double chains (figure 4(b)), similar to those in LiV_2O_5 [14].

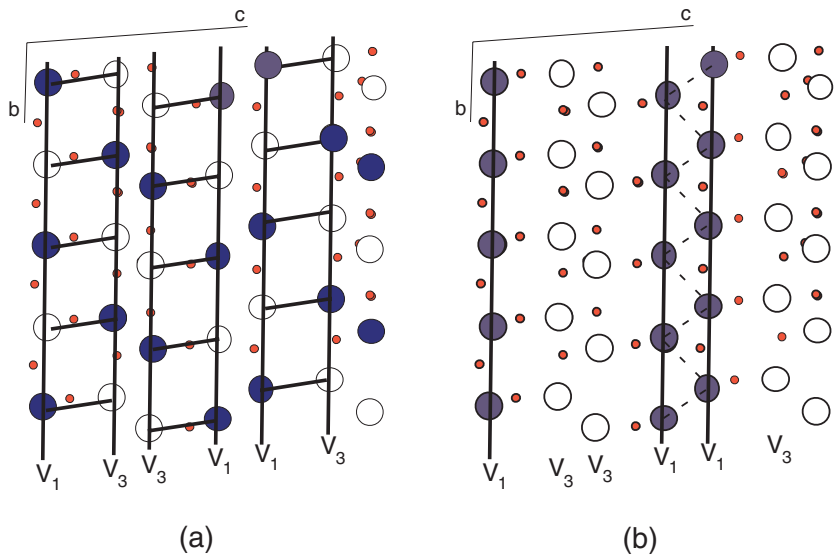

Figure 4. Possible charge ordering patterns in β-$Ca_{0.33}V_2O_5$. (a) Asymmetric spin-ladder structure with a zigzag charge ordering. (b) 1D double-V_1-zigzag-chain (zigzag-ladder) charge ordering.

The Madelung energy calculation [15] for β-$A_{0.33}V_2O_5$ revealed that the lowest-energy configuration of the d electrons is that in which 1D V_1 chains form at half-filling where the A are divalent cations. However, from the comparison between the low-temperature Raman spectra of β-$Ca_{0.33}V_2O_5$, α'-NaV_2O_5 (figure 2), and LiV_2O_5 (figure 3 in [14]), it is difficult to reach an unambiguous conclusion as regards which CO pattern is realized in the low-temperature phase of β-$Ca_{0.33}V_2O_5$. The difficulty arises because of the lack of complete knowledge of phonon dispersions (lack of an appropriate single crystal). As discussed in [16], from the measurements of all inequivalent polarized Raman and infrared spectra it is possible to exclude the possibility of some of the CO patterns. However, even then, additional problems, that complicate the assignment, may arise from the strong resonant effects [17]. Thus, we can suggest optical measurements (ellipsometry) as an appropriate method for distinguishing between these two CO configurations. That is, the presence (or absence) of the $\sim$1.1 eV peak [18] (see also figure 3 in [19]) in the absorption spectra of β-$Ca_{0.33}V_2O_5$ along the b-axis should confirm a 'zigzag' (or double-chain) charge ordering pattern. At the moment, such measurements are not possible, because of the lack of single-crystal samples.

In conclusion, the Raman scattering spectra of β-$Ca_{0.33}V_2O_5$ above and below the phase transition temperature of about 150 K show changes in the phononic and electronic excitations similar to those for α'-NaV_2O_5. At temperatures above the phase transition temperature, the broadening and the asymmetry of the 441 cm^{-1} mode suggest that the electrons are delocalized into the V_1–O_5–V_3 orbitals. Below the phase transition, charge ordering takes place, and the d electrons order either in a 'zigzag' fashion along V_1–V_3 ladders, or at double-chain V_1 ions.

ZVP and MJK acknowledges support from the Research Council of the K U Leuven and DWTC. The work at the K U Leuven is supported by the Belgian IUAP and Flemish FWO and GOA programmes.

References

[1] Yamada H and Ueda Y 1999 *J. Phys. Soc. Japan* **68** 2735
Yamada H and Ueda Y 2000 *J. Phys. Soc. Japan* **69** 1437
[2] Ueda Y, Yamada H, Isobe M and Yamauchi T 2001 *J. Alloys Compounds* **317/318** 109
[3] Obermeier G, Ciesla D, Klimm S and Horn S 2002 *Phys. Rev.* B **66** 085117
[4] Vasil'ev A N, Marchenko V I, Smirnov A I, Sosin S S, Yamada H and Ueda Y 2002 *Phys. Rev.* B **64** 174403
[5] Yamauchi T, Ueda Y and Mori N 2002 *Phys. Rev. Lett.* **89** 057002
[6] Ueda Y, Isobe M and Yamauchi T 2002 *J. Phys. Chem. Solids* **63** 951
[7] Bouloux J C, Galy J and Hagenmuller P 1974 *Rev. Chim. Miner.* **11** 48
[8] Isobe M and Ueda Y 2000 *Mol. Cryst. Liq. Cryst.* **341** 1075
Yamura J I, Isobe M, Yamada H, Yamauchi T and Ueda Y 2002 *J. Phys. Chem. Solids* **63** 957
[9] Itoh M, Akimoto N, Tsuchiya M, Yamada H, Isobe M and Ueda Y 2000 *Physica* B **281/282** 606
Itoh M, Akimoto N, Yamada H, Isobe M and Ueda Y 2001 *J. Phys. Chem. Solids* **62** 351
[10] Déramond E, Savariault J M and Galy J 1994 *Acta Crystallogr.* C **50** 164
[11] Popović Z V, Konstantinović M J, Gajić R, Popov V N, Isobe M, Ueda Y and Moshchalkov V V 2002 *Phys. Rev.* B **65** 184303
[12] Popović Z V, Konstantinović M J, Gajić R, Popov V, Raptis Y S, Vasil'ev A N, Isobe M and Ueda Y 1999 *Solid State Commun.* **110** 381
[13] Loa I, Schwarz U, Hanfland M, Kremer R K and Syassen K 1999 *Phys. Status Solidi* b **215** 709
[14] Popović Z V, Gajić R, Konstantinović M J, Provoost R, Moshchalkov V V, Vasil'ev A, Isobe M and Ueda Y 2000 *Phys. Rev.* B **61** 11454
[15] Nishimoto S and Ohta Y 2001 *J. Phys. Soc. Japan* **70** 309
[16] Konstantinović M J, Popović Z V, Vasil'ev A N, Isobe M and Ueda Y 1999 *Solid State Commun.* **112** 397
[17] Konstantinović M J, Popović Z V, Moshchalkov V V, Presura C, Gajić R, Isobe M and Ueda Y 2002 *Phys. Rev.* B **65** 245103
[18] Konstantinović M J, Dong J, Ziaei M E, Clayman B P, Irwin J C, Yakushi K, Isobe M and Ueda Y 2001 *Phys. Rev.* B **63** 121102(R)
[19] Hübsch A, Waidacher C and Becker K W 2001 *Phys. Rev.* B **64** 241103(R)